AD_____

MIPR NUMBER 96MM6643

TITLE: Whole Body Center of Gravity and Moments of Inertia Study

PRINCIPAL INVESTIGATOR: Rebecca B. Schultz, Louise A. Obergefell, Annette Rizer, Christopher B. Albery

CONTRACTING ORGANIZATION: Armstrong Laboratory
Brooks AFB, Texas 78235-5118

REPORT DATE: December 1996

TYPE OF REPORT: Final

PREPARED FOR: Commander
U.S. Army Medical Research and Materiel Command
Fort Detrick, Frederick, Maryland 21702-5012

REPORT DOCUMENTATION PAGE

Form Approved
OMB No. 0704-0188

1. AGENCY USE ONLY *(Leave blank)*	2. REPORT DATE	3. REPORT TYPE AND DATES COVERED
	December 1996	FINAL (15 Dec 95 - 31 Dec 96)

4. TITLE AND SUBTITLE
Whole Body Center of Gravity and Moments of Inertia Study

5. FUNDING NUMBERS
96MM6643

6. AUTHOR(S)
Rebecca B. Schultz, Louise A. Obergefell, Annette Rizer, Christopher B. Albery

7. PERFORMING ORGANIZATION NAME(S) AND ADDRESS(ES)
Armstrong Laboratory
Brooks AFB, Texas 78235-5118

8. PERFORMING ORGANIZATION REPORT NUMBER

9. SPONSORING/MONITORING AGENCY NAME(S) AND ADDRESS(ES)
Commander
U.S. Army Medical Research and Materiel Command
Fort Detrick, Frederick, Maryland 21702-5012

10. SPONSORING/MONITORING AGENCY REPORT NUMBER

11. SUPPLEMENTARY NOTES

12a. DISTRIBUTION / AVAILABILITY STATEMENT
Approved for public release; distribution unlimited

12b. DISTRIBUTION CODE

13. ABSTRACT *(Maximum 200)*

With the inclusion of women in combat aircraft, the question of safe ejection seat operation is raised. The population of combat pilots now includes much smaller ejection seat occupants, which could significantly effect seat performance. The objective of this study is to measure human whole-body center of gravity (CG) locations and moments of inertia (MOI) on 69 subjects who anthropometrically represent the possible future pilot population (98-245 pounds). A procedure has been developed to measure human whole-body CG and MOI in a seated position using a Space Electronics Mass Properties Instrument. MOI of a subject is measured along six different axes: the three primary axes X (chair on back), Y (chair on right-hand side), and Z (chair upright), and three off-axes positions XY, YZ, and XZ with the chair at a 45 degree angle between the primary axes. Accuracy and repeatability testing have shown this procedure is having approximately 2-5% error. Data collected from this study is being used to validate the Articulated Total Body (ATB) model for use as a predictive tool. In addition, it will be used to provide criteria for use of Air Force and Navy ejection seats by the expanded population.

14. SUBJECT TERMS
Defense Women's Health
Center of Gravity, Moments of Inertia, Whole-Body, Human, Ejection Seat, Model

15. NUMBER OF PAGES
36

16. PRICE CODE

17. SECURITY CLASSIFICATION OF REPORT	18. SECURITY CLASSIFICATION OF THIS PAGE	19. SECURITY CLASSIFICATION OF ABSTRACT	20. LIMITATION OF ABSTRACT
Unclassified	Unclassified	Unclassified	Unlimited

FOREWORD

Opinions, interpretations, conclusions and recommendations are those of the author and are not necessarily endorsed by the U.S. Army.

____ Where copyrighted material is quoted, permission has been obtained to use such material.

____ Where material from documents designated for limited distribution is quoted, permission has been obtained to use the material.

RBD Citations of commercial organizations and trade names in this report do not constitute an official Department of Army endorsement or approval of the products or services of these organizations.

____ In conducting research using animals, the investigator(s) adhered to the "Guide for the Care and Use of Laboratory Animals," prepared by the Committee on Care and use of Laboratory Animals of the Institute of Laboratory Resources, national Research Council (NIH Publication No. 86-23, Revised 1985).

RBD For the protection of human subjects, the investigator(s) adhered to policies of applicable Federal Law 45 CFR 46.

____ In conducting research utilizing recombinant DNA technology, the investigator(s) adhered to current guidelines promulgated by the National Institutes of Health.

____ In the conduct of research utilizing recombinant DNA, the investigator(s) adhered to the NIH Guidelines for Research Involving Recombinant DNA Molecules.

____ In the conduct of research involving hazardous organisms, the investigator(s) adhered to the CDC-NIH Guide for Biosafety in Microbiological and Biomedical Laboratories.

Rebecca B Doherty 23 Dec 96

PI - Signature Date

TABLE OF CONTENTS

INTRODUCTION

On 28 April 1993, the Secretary of Defense lifted restrictions preventing women from flying combat aircraft. Shortly thereafter, women were flying ejection-seat-equipped aircraft. Specifications for selection of the next generation training system were changed to accommodate the future pilot population. Congress, on at least two occasions[1,2], has requested the Air Force and the Navy to pursue the safety and accommodation issues with regard to this expanded population, particularly with regard to ejection seat performance. The expanded population may allow at least 82% of the female population as well as males on both the smaller and larger anthropometric extremes to be potential ejection seat users[3].

Ejection safety is a critical issue for accommodating the potential future pilot population. All operational ejection seats in service for the Navy and Air Force were designed to accommodate a nude male weight range of approximately 135-220 pounds. The new expanded population may stretch the weight range at both the lower and higher ends to 98-245 pounds. Similarly, sitting height restrictions may be loosened to allow shorter people to fly. Ejection seat performance depends largely on the occupant's size and weight. More specifically, occupant mass, center of gravity (CG), and mass distribution have a direct effect on ejection accelerations and forces, seat stability and control, harness fit, parachute opening shock, and spinal injury potential. Occupants at the heavier end of the anthropometric continuum may not have enough catapult force to completely clear the aircraft[3].

As computer technology has matured over the past several decades, so too have the analytical, geometrical, and mathematical human dynamic and ejection seat performance models. With modern computing horsepower, predicting total body CG and moments of inertia (MOI) is becoming simpler and more accurate[4]. Mathematical modeling and computer simulations of the crew member during ejection and other impact events can provide valuable insight into the biodynamic responses of a crew member[5]. For instance, the Articulated Total Body (ATB) model, developed by the Armstrong Laboratory (AL), is used by the Air Force to predict human body responses to forces encountered during an ejection and other hazardous force exposures. This model takes input CG and MOI data from 17 body segments and outputs calculated net or whole-body inertial properties, thus enabling the prediction of biodynamic responses of the occupant duing an ejection. While the analytical process for calculating the net inertial properties has been verified, validation against empirical data has yet to be completed. Once the validation is completed, the ATB model may be used to predict net inertial properties of a broad range of seat occupants in various seat configurations and also conduct dynamic simulation of the ejection seat with an occupant[6]. Another model used by AL is the Generator of Body Data (GEBOD) which allows for the generating of human or dummy data for ATB simulations. Mass properties, joint locations, segment geometry, and mechanical properties can be calculated using GEBOD. Additional models which may benefit from

this study's data include the six degrees-of-freedom simulation models, such as the EASY5X computer model used by the Air Force's Wright Laboratory, which models the Air Force's Advanced Concept Ejection Seat (ACES II) performance, and the Navy's trajectory simulation model for the Navy Aircrew Common Ejection Seat (NACES).

In order to determine the range of whole-body inertial properties, Armstrong Laboratory is conducting an intensive study to determine human body CGs and MOIs on a subject population anthropometrically representative of the population to be accommodated by the Joint Primary Aircraft Training System (JPATS). These data will then be used to validate the Articulated Total Body (ATB) model, which will be used to predict human whole-body inertial properties for any body orientation or position.

HUMAN TESTING

Measurement System

The Automated Mass Properties Measurement System, developed at the Armstrong Laboratory, provides an accurate and efficient means of measuring mass, center of gravity location, and mass moments of inertia. This procedure has been used to test complete manikins and individual manikin segments, including the Advanced Dynamic Anthropomorphic Manikin (ADAM), Sea Water Instrumented Manikin (SWIM), Hybrid III 5th, 50th, and 95th percentile male and 5th percentile female dummies, Side Impact Dummy (SID) and a nine-month-old infant dummy. Various helmet systems and Night Vision Goggles (NVG), such as the HGU -5/P, -26/P, -53/P, -55/P, -68/P, -86/P, -87/P, Combat Edge, Eagle Eyes, Cats Eyes, Anvis, Merlin, and I-Nights systems have also been tested. The results of these studies have been compiled into databases which have been used in computer models to assess the effectiveness of vehicle safety designs and to study human responses to various head encumbering equipment. This data has also been used by review boards for the assessment of flight safety and establishing criteria for allowable added head mass. A complete description of testing the procedures used in these programs are described in "The Standard Automated Mass Properties (STAMP) Testing and Calibration Procedure."[8] For the testing of human, whole-body properties, these procedures were somewhat modified and implemented.

The equipment used for determining the mass properties of the human subject includes a moment table, electronic balance, adjustable stand, lightweight seat and holding box, Space Electronics Mass Properties Instrument, positioning platter, electronic position coordinate digitizer, computer, associated software, electronic hoist, gantry, leveling boom, and fixed and variable length lifting straps. Figure 1 shows the set-up and equipment used for the Human Mass Properties Study.

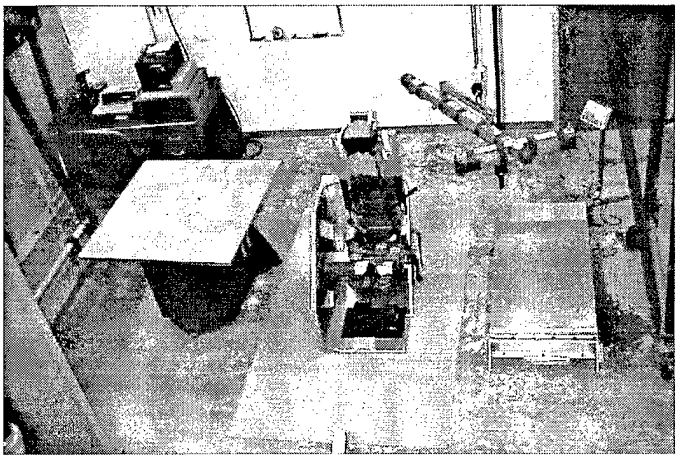

Figure 1: Mass Properties Set-Up for Human Mass Properties Study.

Subject Selection

Subjects were selected in order to be representative of a subgroup to the 1988 Army samples of men and women.[9] The samples were constructed to represent Air Force demographic requirements (age, race, height, and weight) listed in AFI 48-123 and resulted in sample sizes of 1,301 males and 851 females. The variables used to select subjects for this study were sitting height, stature and weight. Potential subjects were compared to the 1988 subgroup on these variables. A bivariate stature and weight plot was created. The stature and weight of the volunteers for this study were plotted on an overlaid plot to ensure the volunteer subject pool matched the sample distribution. The procedure was repeated for sitting height and stature. Figures 2 through 5 show these bivariate plots for males and females.

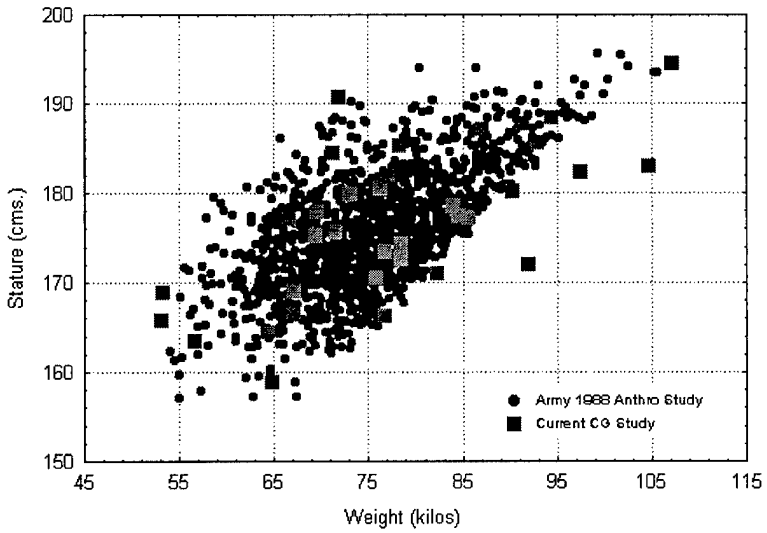

Figure 2: Males: Stature vs Weight.

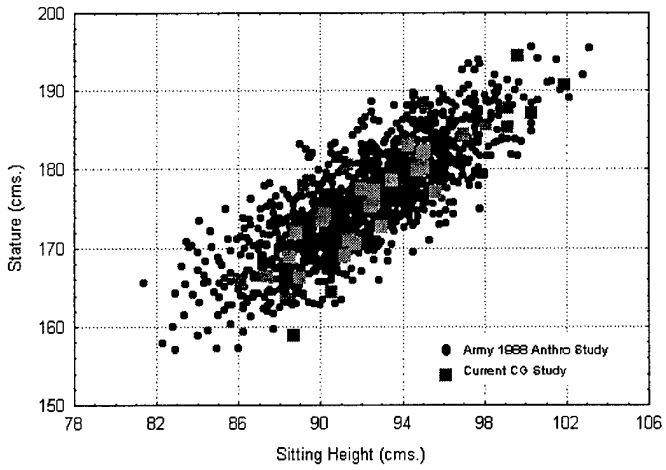

Figure 3: Males: Stature vs Sitting Height.

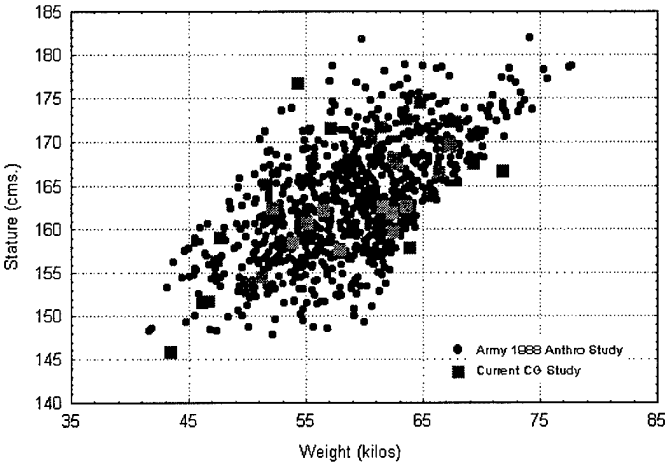

Figure 4: Females: Stature vs Weight.

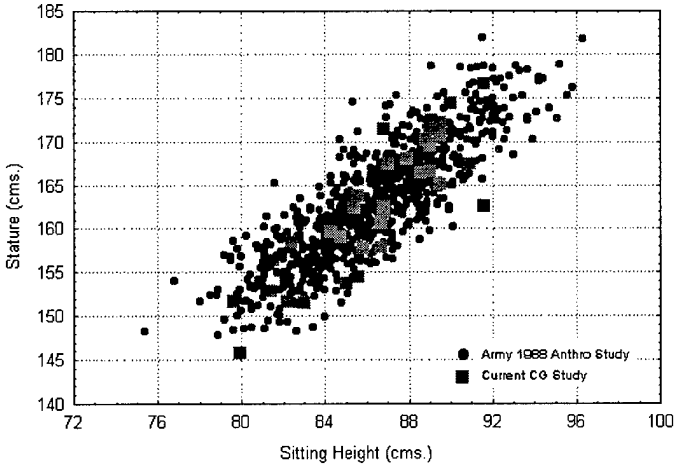

Figure 5: Females: Stature vs Sitting Height.

Subjects were solicited from local universities and Wright-Patterson Air Force Base personnel. All subjects participating in the study were volunteers, with no required technical qualifications or special training. As required, the entire procedure was first approved by the Human Use Review Committee (HURC). All subjects were first asked to read and sign the informed consent forms before beginning with the anthropometric measurements and again before the commencement of the mass properties data collection. These forms explained the procedures and risks involved in the studies. The subjects were first screened for height and weight, and, in order to participate, had to meet the established stature versus weight criteria used for entry into an aviation program. The subjects were asked to wear shorts, T-shirt, and socks only.

A total of 70 male and female subjects were selected for testing, 69 were measured for CG and MOI (one subject dropped out of the study). Table 1 shows the average age, weight and height of the subjects. Subject weight ranged from 97 pounds to 236 pounds.

Table 1: Average Subject Age, Weight and Height.

	Number of Subjects	Age	Weight (kgs)	Height (cm)
Male	35	29	78.5	176.8
Female	34	27	58.5	162.5
Total	69	28	68.6	169.8

Anthropometric Measurements

Thirty-eight detailed anthropometric measurements were recorded for each subject by the Computerized Anthropology Research & Design (CARD) Lab of the Design Technology Branch, Armstrong Laboratory using standard instruments (anthropometer, spreading and sliding calipers, and tape). Researchers relied on well-defined landmarks to place the tools for each measurement. The landmark technician located the landmarks by palpating the subject and marking the landmarks clearly with a make-up pencil. The measurement technician used these marks as a guide for tool placement. These detailed measurements serve as the input data required for the GEBOD model. Table 2 provides a listing of the anthropometric measurements that were taken on each subject.

Table 2: Anthropometric Measurements.

Weight	Stature	Acromion Height
Axilla Height	Waist Height	Neck Circumference
Forearm Circumference	Elbow Circumference	Biceps Circumference (extended and flexed)
Wrist Circumference	Thigh Circumference	Foot Breadth
Lateral Malleolus Height	Sitting Height	Eye Height, Sitting
Acromion Height, Sitting	Knee Height, Sitting	Buttock/Knee Length
Lateral Malleolus Height	Knee Circumference	Calf Circumference
Ankle Circumference	Chest Depth	Waist Depth
Hip Depth	Biacromial Breadth	Chest Breadth
Waist Breadth	Hip Breadth	Shoulder/Elbow Length
Forearm/Hand Length	Foot Length	Menton-to-Top of Head Length
Head Length	Hand Length	Hand Depth
Hand Breadth		

Fitting of Subject within the Lightweight Seat and Holding Box

The lightweight seat and three-sided holding box were designed to hold the subject during testing and to provide a Cartesian coordinate system which allows transformation of properties measured with respect to the box axis system to a predetermined seat coordinate system. The box was constructed of riveted sheets of thin, perforated aluminum, providing a rigid, but very lightweight structure. The lightweight seat was designed to accommodate the population of interest. It had adjustable seat pan height and depth, and adjustable Velcro and buckle-type straps to secure the subject within the seat. As shown in Figure 6, the subject was placed in the seat such that the subject's upper legs were parallel to the XY-plane (floor), and at 90-degrees to the lower legs. The upper arms were kept alongside of the upper torso and held against the seat-back. The lower arm were positioned such that the hands rested comfortably on the upper legs. Upper leg and lower arm angular pitch position was recorded, along with lower arm yaw. These positions are important for the GEBOD and ATB models. The subject wore a HGU-55/P helmet and visor assembly, which held the subject's head and neck in position and provided protection. Upon completion of securing the subject within the seat, the measurement process was initiated.

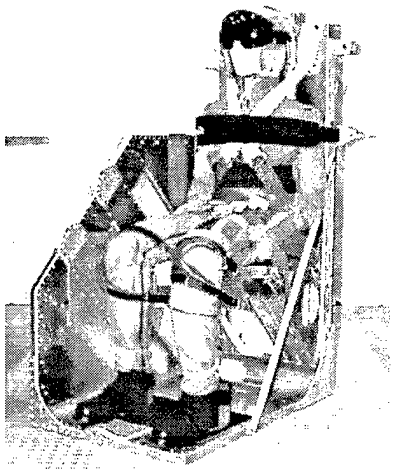

Figure 6: Manikin Secured in Lightweight Chair.

Weight and Center of Gravity Determination

The weight and CG location were determined with the use of an electronic balance and moment table assembly. The subject within the holding fixture (referred to as the composite) was hoisted onto the electronic balance, and the weight was recorded. The moment table assembly was then placed on the electronic balance and adjustable stand. The composite's CGs about the box X (composite facing forward, in an upright position), Y (composite rotated 90-degrees, in an upright position), and Z (composite set on its back) axes were then recorded by hoisting and rotating the composite about the respective axis. Figure 7 shows the electronic balance and moment table assembly loaded with the composite in the CG_x measurement configuration. The free body diagram of this assembly is shown in Figure 8.

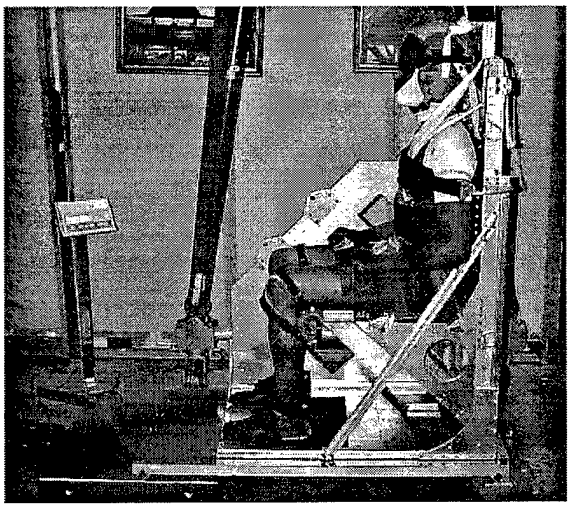

Figure 7: Measurement of the CG about the x-axis.

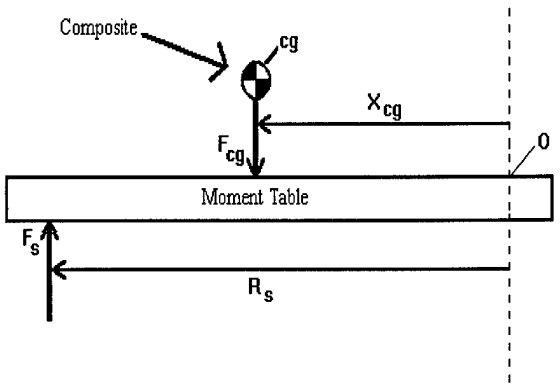

Figure 8: Free Body Diagram of "Loaded" Moment Table.

After taring the weight of the moment table, the moment balance equation for the composite for the X direction is:

$$\sum M_O = F_S R_S - F_{CG} X_{CG} = 0 \quad (1)$$

or

$$F_S R_S = F_{CG} X_{CG} \quad (2)$$

where,

$$F_{CG} = Mg \quad (3)$$

and M is the mass of the composite. Solving for X_{CG} we get

$$X_{CG} = \frac{F_S R_S}{F_{CG}} \quad (4)$$

The same procedure is used to calculate CG_y and CG_z.

To determine the center of gravity of the human subject alone, the entire procedure was repeated for the empty seat. The empty seat CG was then subtracted from the composite data, resulting in the CG of the human subject in a seated position. The total moment due to the composite is

$$F_{CG} X_{CG} = F_B X_B + F_T X_T \quad (5)$$

and solving for X_T we get

$$X_T = \frac{F_{CG} X_{CG} - F_B X_B}{F_T} \quad (6)$$

where,

F_B	=	Weight of Lightweight Seat and Box
F_T	=	Weight of Human
F_{CG}	=	Weight of Composite
X_B	=	CG location of Lightweight Seat and Box
X_T	=	CG location of Human Subject
X_{CG}	=	CG location of Composite.

This provides the CG of the human subject with respect to the axis system of the box. The same procedure is used to determine Y_T and Z_T.

Upon completion of the CG measurements and calculations, the composite was hoisted onto the Space Electronics Mass Properties Instrument.

Moments of Inertia Determination

Measurement of the moments of inertia of a subject secured within the lightweight seat and box was accomplished using the Space Electronics Mass Properties Instrument, Model KGR 8945. This instrument is based on a torsional pendulum technique. A torsional pendulum, illustrated in Figure 9, consists of a disk that is attached to a vertical shaft that is fixed at the bottom end and can be induced to oscillate about the shaft.

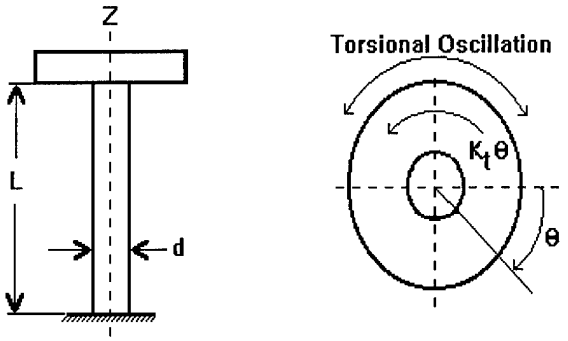

Figure 9: Torsional Pendulum

If the disk is given an angular displacement, θ, from its equilibrium position and released, it will oscillate due to the restoring torque, T, exerted by the shaft. The magnitude of T is given by

$$T = \frac{GJ}{L}\theta = K_t\theta \tag{7}$$

where K_t is the torsional spring constant of the shaft and is a function of the shear modulus, G, the length of the shaft, L, and the polar moment of inertia, J, of the cross section of the shaft.

If the torsional moment of inertia of the disk is I and the torsional force acts to bring the system back to equilibrium, then we can write

$$-K_t\theta = I\frac{d^2\theta}{dt^2}. \tag{8}$$

Equation 8 can also be written as

$$\frac{d^2\theta}{dt^2} + \frac{K_t}{I}\theta = 0 \tag{9}$$

which is a homogenous differential equation for which the solution is

$$\theta = C_1 \cos\sqrt{\frac{K_t}{I}}t + C_2 \sin\sqrt{\frac{K_t}{I}}t \qquad \textbf{(10)}$$

where C_1 and C_2 are constants which can be determined from the initial conditions. If the initial conditions are

$$\theta \text{ at } t \;=\; 0 \text{ equals } 0$$

and **(11)**

$$\theta \text{ at } t \;=\; \frac{\pi}{2}\sqrt{\frac{I}{K_t}} \text{ equals } A$$

then

$$C_1 = 0, \qquad C_2 = A \qquad \textbf{(12)}$$

and equation 10 becomes

$$\theta = A\sin\sqrt{\frac{K_t}{I}}t. \qquad \textbf{(13)}$$

Equation 13 is the equation for simple harmonic motion in which $\sqrt{\frac{K_t}{I}}$ is the angular frequency, ω_n, at which the disk and shaft oscillate in radians per second. The period of oscillation, τ_n, is given by

$$\tau_n = \frac{1}{\omega_n} = \sqrt{\frac{I}{K_t}}. \qquad \textbf{(14)}$$

Solving equation 14 for the moment of inertia gives

$$I \;=\; K_t\tau_n^2. \qquad \textbf{(15)}$$

Equation 15 shows that the moment of inertia is directly proportional to the square of the period of the rotational oscillation with the proportionality constant being the torsional spring constant. The period of the oscillations are measured by using a photocell device. To ensure that only rotational motion of the pendulum occurs about the fixed pendulum axis (through the centroid of the platter), the instrument rides on a spherical gas bearing.

The proportionality constant, K_t, of the pendulum is a function of the torsional stiffness and length of the torsion rod. The instrument measures center of gravity and moments of inertia about the torsional pendulum axis. The moment measured is that of the pendulum itself, plus the pendulum platform, and the composite set upon the pendulum platform. The pendulum platform consisted of a 4'x4'x2" honeycomb and aluminum gridded platter. This platter was made specifically for this study to allow for accurate, safe, and convenient placement of the composite.

Although the instrument has the capability to measure the CG position of items on the platform, it functions most accurately when the CG position of the object being tested is closely aligned with the fixed pendulum axis. Therefore, the standard procedure was to mount the composite on the gridded test platter so that the horizontal CG position of the composite was within +/- 0.1 inches of the pendulum vertical axis. Once the composite was in place, the CG was again measured, this time with the use of the mass properties instrument. This was to ensure the subject had not shifted, or the experimenter had erroneously placed the composite on the platter. If either of the two had occurred, and the composite's CG was detected to be out-of-tolerance, the computer notified the experimenter with a message prompting the experimenter to reposition the composite. Additionally, the recorded CG of the composite on the instrument was used to calculate the MOI through the CG of the composite. This process was repeated for all six MOI's, with the composite being reoriented between each measurement.

The rotational inertial properties of the composite can be expressed by an inertia tensor. The tensor values depend on the coordinate system origin and orientation with respect to which the tensor is calculated. Moment of inertia measurements were taken about six different axes to generate an inertia tensor from which the orientation of the principal axes and the magnitudes of the principal moments of inertia were determined. For simplicity, three of the axes chosen (X, Y, Z) were about the cardinal axes (box edges) of the holding box. The remaining three axes (XY, YZ, XZ) were axes in the planes of the three walls of the holding box at 45-degree angles to the cardinal axes. These 45-degree measurements utilized a custom made lightweight jig. All six axes intersect at the origin of the coordinate system of the box.

In order to measure a moment about any given axis, that axis must be normal to the pendulum test platter. With the cardinal axes (X, Y, Z) this presented no problem since placing the box on any one of its three sides caused one axis to be normal to the platter. Figure 10 shows the composite being measured about the Z-Axis.

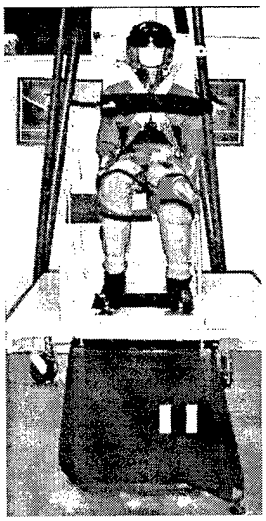

Figure 10: Measurement of MOI about the Z-axis.

With the noncardinal axes, however, it was necessary to utilize a jig which, when placed on the pendulum surface, aligned two of the cardinal planes at an angle of 45-degrees to the horizontal platter. In this way, the other axis which is at 45-degrees to the cardinal axes is aligned normal to the platter surface as shown in Figure 11.

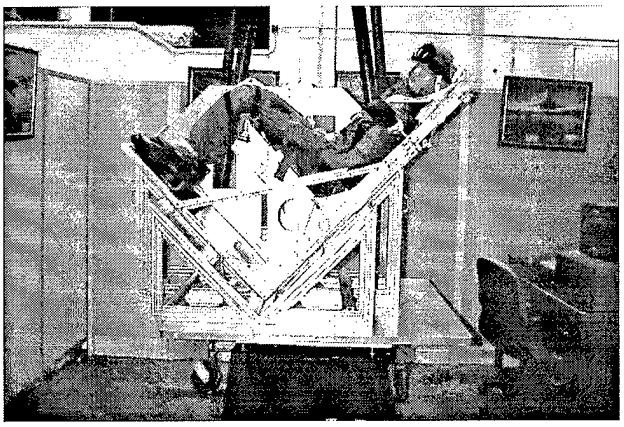

Figure 11: Measurement of MOI about the XZ Axis.

From these six moment of inertia measurements, the products of inertia were determined from the equation

$$P_{ab} = \frac{I_a + I_b \tan^2 \theta - (1 + \tan^2 \theta) I_{ab}}{2 \tan \theta} \qquad \textbf{(16)}$$

where, P_{ab} = the product of inertia in the ab plane
I_a = the moment of inertia about the cardinal axis a
I_b = the moment of inertia about the cardinal axis b
I_{ab} = the moment of inertia about the noncardinal axis in the ab plane
θ = the angle between the axis a and axis b.

Because the angle between axes is 45-degrees, equation 16 simplifies to

$$P_{ab} = \frac{I_a + I_b - 2I_{ab}}{2} \quad . \qquad \textbf{(17)}$$

Upon completion of the six moment measurements with the composite, the entire procedure was repeated with the empty lightweight seat and box. Various sized balloons were inserted to ensure the holding straps were in the same orientation as when measured with the subject. The lightweight seat, box, and jig inertial properties are subtracted from the measured composite properties using the parallel axis theorem.

The resulting inertia tensor, which is with respect to the center of mass of the test object, may be written as

$$\underline{T} = \begin{bmatrix} I_X & -P_{XY} & -P_{XZ} \\ -P_{YX} & I_Y & -P_{YZ} \\ -P_{ZX} & -P_{ZY} & I_Z \end{bmatrix}. \quad \textbf{(18)}$$

This inertia tensor is symetric and can be reduced to diagonal form in which the products equal zero and the diagonal elements are the principal moments. This is accomplished by determining the values of λ which satisfy the equation

$$(\underline{T} - \underline{I}\lambda)\omega = 0. \quad \textbf{(19)}$$

$\underline{I}$ are the principal moments of inertia. The vectors associated with these values are the directions of the principal axes associated with the principal moments of inertia. These vectors, expressed as a matrix of cosines, define the directions of the principal axes with respect to the axis parallel to the box axis system, but are centered at the subject's center of mass.

Coordinate System Transformation

To this point, all measurements have been located with respect to the box coordinate axes. To reference the properties of the subject to a seat-based coordinate system, subject and seat landmarks were digitized with respect to the box axis system using the electronic position coordinate digitizer shown in Figure 12.

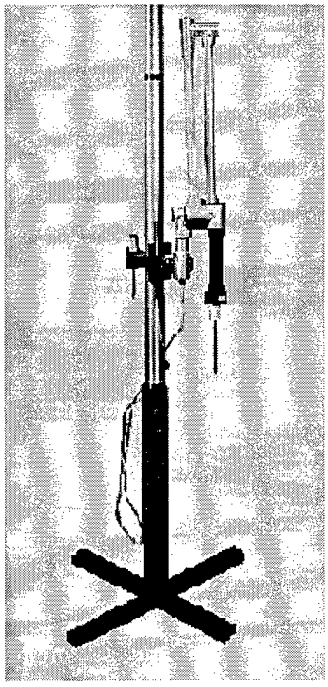

Figure 12: Electronic Position Coordinate Digitizer.

The box origin, located at the rear and right hand corner of the outer box, and points representing the X, Y, and Z axes of the box were digitized along with three landmarks located on the seat, along with the subject's omphalion (belly-button) . These three seat landmarks define the axis system of the seat with respect to the holding box axes. The seat's origin is located at the Seat Reference Point (SRP), which is located at the intersection of the seat back, seat pan, and the midline of the seat. With the origin at the SRP, the positive Z-axis extends in the upward direction along the seat-back, the positive X-axis extends in the forward direction parallel to the seat pan, and the positive Y-axis extends to the left. This specifies a transformation matrix which is multiplied by the principal axis cosine matrix to produce a transformation matrix from the principal axes to the seat axis system.

This transformation process is performed according to

$$[A_{tp}] = [A_{tb}]\,[A_{pb}]^T \qquad \textbf{(20)}$$

where, $[A_{tp}]$ = Transformation cosine matrix from principal to seat axis system
$[A_{tb}]$ = Transformation cosine matrix from box to seat axis system
$[A_{pb}]^T$ = Transpose of transformation matrix from box to principal axis system.

The inertia tensor is then transformed to the seat coordinate system by performing a similarity transformation according to

$$[I^{(t)}] = [A_{tp}]\,[I^{(p)}]\,[A_{tp}]^T \qquad \textbf{(21)}$$

where, $[I^{(t)}]$ = Inertia tensor in the seat axis system
$[I^{(p)}]$ = Principal moments of inertia
$[A_{tp}]$ = Transformation matrix from the principal to seat axis system
$[A_{tp}]^T$ = Transpose of transformation matrix A_{tp}.

The origin of the seat axis system was chosen to remain at the SRP rather than at the center of mass, but may be located at some arbitrary point with the center of mass of the subject given in terms of this new origin by simple vector operations. By convention, the principal moment values are defined with respect to the subject's center of mass.

Accuracy and Repeatability Tests

Before testing human subjects, accuracy and repeatability testing for the mass properties measurement system were performed[10]. A 68.0 kg, homogeneous, rectilinear calibration steel slug was used as the first test object. The slug was strapped into the lightweight chair and CG and MOI measurements were taken along the six different axes using the mass properties instrument. These six moments were used to calculate an inertia tensor from which the principal moments were computed. This process was repeated three times. Since this was a homogenous, symmetric object, its principal moments of inertia could be easily calculated for comparison to the measured values (Table 3). The X

principal moment had less then 0.5% error. The Y principal moment had an error of about 4%. Since the calibration slug was tall and thin and the chair was designed to support a human, the slug slipped slightly when turned on its side, which could explain this larger error. The Z principal MOI had approximately a 5% error. This Z moment was much smaller than the other two moments, therefore the differences in these values result in larger percentage differences than for the larger moments.

Table 3: Accuracy Test: Calibration Slug.

	Principal MOI	(kg-cm^2)
Calibration Slug Calculated Values	X:	27986
	Y:	28594
	Z:	1505
Calibration Slug Experimental Values	X:	28109
	Y:	27444
	Z:	1583
Percent Error	X:	0.44%
	Y:	4.02%
	Z:	5.18%

In order to test an object with three moments of an equivalent order of magnitude, a 64.0 kg wood and concrete calibration slug was made. The wood and concrete slug was strapped into the chair and CG and MOI measurements were taken using the mass properties instrument. This was repeated twice. Calculations were done by adding the CG and MOI from a solid concrete block within a hollow wooden shell[11]. The X and Y principal moments had less than 2% error, while the Z moment (still the smallest) had an error of approximately 4% (Table 4).

Table 4: Accuracy Test: Concrete and Wood Block.

	Principal MOI	(kg-cm^2)
Concrete/Wood Block Calculated Values	X:	12845
	Y:	11756
	Z:	8095
Concrete/Wood Block Experimental Values	X:	13020
	Y:	11825
	Z:	8428
Percent Error	X:	1.36%
	Y:	0.59%
	Z:	4.11%

A repeatability test was performed using a human subject weighing 72.4 kg. Three complete sets of measurements were performed over two consecutive days. The subject was secured in the chair and CG and MOI measurements were taken using the mass properties instrument. The mean, standard deviation, and coefficient of variance were computed for the CG, MOI, and direction cosine angles for the principal axes and are shown in Table 5. The X, Y, and Z CGs had a coefficient of variance of 1% or less. The X, Y, and Z MOIs had a coefficient of variance of less than 2%. The direction cosine angles for the principal axes showed notable variability, especially for the X and Y axes. Since the X and Y MOIs are very similar, the X and Y direction cosine angles are very sensitive to small differences in moment magnitude and therefore are expected to exhibit a large amount of variability. The Z cosine angle, on the other hand, is much more stable.

Table 5: Repeatability Test: Human Subject.

	CG (cm)		Principal MOI ($kg\text{-}cm^2$)		Direction Cosine (degrees)	
Subject Test #1	:	28.51	X:	68924	α:	42.69
	:	38.72	Y:	69804	β:	34.92
	z:	69.83	Z:	18581	γ:	26.36
Subject Test #2	x:	29.02	X:	69659	α:	31.24
	y:	38.35	Y:	70074	β:	17.25
	z:	69.83	Z:	19303	γ:	26.10
Subject Test #3	x:	28.00	X:	68712	α:	26.23
	y:	38.88	Y:	69186	β:	0.00
	z:	70.10	Z:	19023	γ:	26.23
Mean(s):	x:	28.66	X:	69098	α:	33.39
	y:	38.65	Y:	69688	β:	17.39
	z:	69.92	Z:	18969	γ:	26.23
Standard Deviation	x:	0.25	X:	405.88	α :	6.89
	y:	0.22	Y:	371.59	β :	14.26
	z:	0.12	Z:	297.49	γ:	0.11
Coefficient of Variance	x:	0.88%	X:	0.59%	α:	20.63%
	y:	0.57%	Y:	0.53%	β:	81.98%
	z:	0.18%	Z:	1.57%	γ:	0.40%

Subject Data

The CG (X, Y, and Z coordinates) was found for each subject based on a coordinate system with the origin at the SRP (Figure 13). Average CGs for the sixty-nine subjects are given in Table 6. Figure 14 is a graph of CG_x and CG_z for each subject. Female subjects' CGs tend to be lower and further back as compared to the male subjects' CGs.

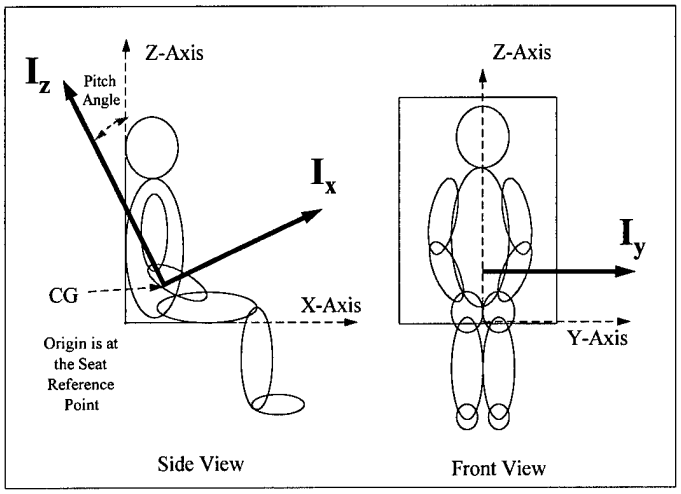

Figure 13: CG and MOI coordinate system.

Table 6: Average Center of Gravities

	CG_x (cm) Avg ± S.D.	CG_y (cm) Avg ± S.D.	CG_z (cm) Avg ± S.D.
Male	23.48 ± 1.4	0.48 ± 0.8	26.22 ± 1.4
Female	22.15 ± 1.3	0.70 ± 0.6	23.43 ± 1.0
All	22.82 ± 1.4	0.59 ± 0.7	24.85 ± 1.8

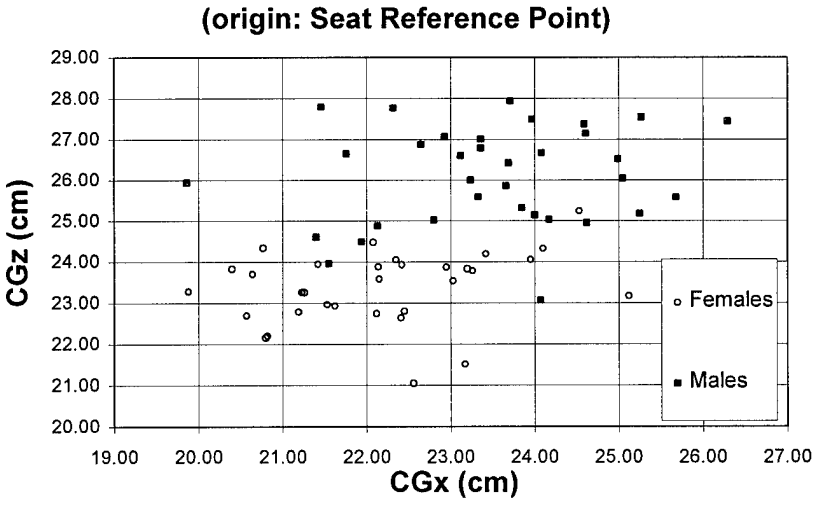

Figure 14: Male vs Female CG_x and CG_z

Principal moments of inertia were calculated based on the six measured MOIs. A summary of these moments are shown in Table 7. Average MOIs for the females were 37%, 34%, and 39% (X, Y and Z, respectively) smaller than the males MOIs, while the female average weight was only 25% smaller and the height only 8% smaller. Figures 15, 16, and 17 show the I_x, I_y, and I_z distributions for males, females, and combined.

Table 7: Average Principal Moments of Inertia

	I_x (kg-cm^2) Avg ± S.D.	I_y (kg-cm^2) Avg ± S.D.	I_z (kg-cm^2) Avg ± S.D.
Male	88478 ± 19472	85859 ± 18147	24100 ± 6181
Female	55719 ± 9976	56796 ± 9370	14764± 2841
All	72336 ± 22584	71538 ± 20530	19499± 4642

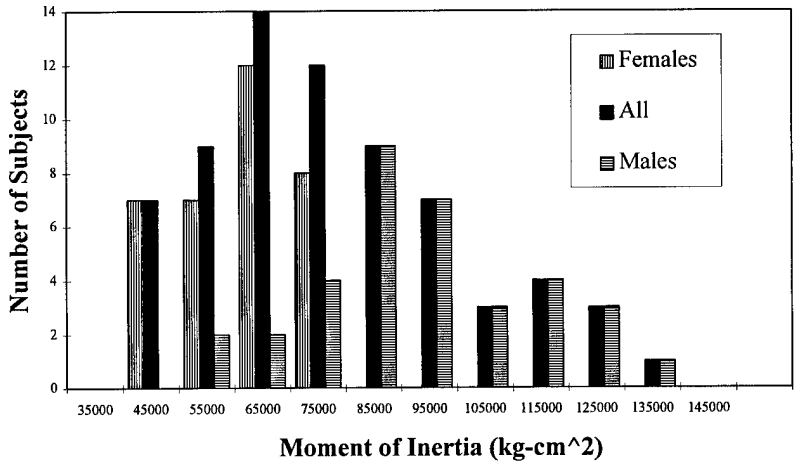

Figure 15: I_x Distribution

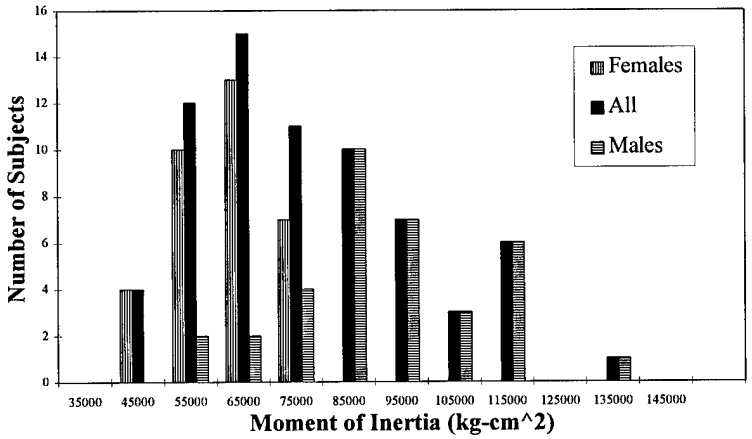

Figure 16: I_y Distribution

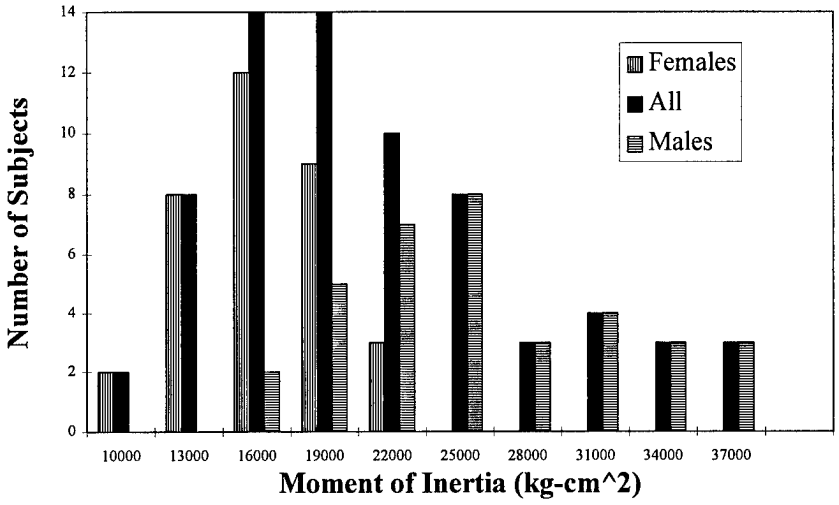

Figure 17: I_z Distribution

MODEL VALIDATION

Multibody dynamics programs for simulating human body response in automobile and aircraft crashes, aircraft ejections, and other dynamic environments require data sets describing the geometry and mass properties of the body. Directly measuring some of these parameters, specifically individual segmental inertial properties, on live humans is inherently impossible. Many indirect methods have been used to estimate these parameters including measuring cadaver segments, stereophotogrammetry, and laser scanning. The Generator of Body Data (GEBOD) program[12] was developed to provide these data sets for the ATB model[13], and was later modified to provide data sets for MADYMO (MAthmatical DYnamical MOdel)[14]. A typical GEBOD data set is illustrated in Figure 18. The data sets include the following for each segment:

segment mass
segment center of gravity (CG) location
segment principal MOIs
orientation of principal axes
surface ellipsoid geometry
joint locations
joint ranges of motion
joint resistive torque properties

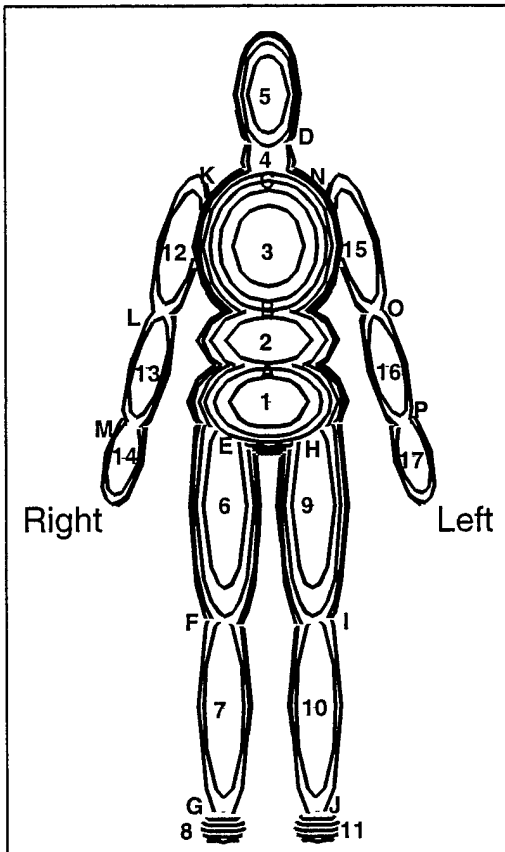

	SEGMENTS		JOINTS
1	Pelvis	A	Pelvis/Abdomen
2	Abdomen	B	Abdomen/Thorax
3	Thorax	C	Neck Pivot
4	Neck	D	Head Pivot
5	Head	E	Right Hip
6	Right Thigh	F	Right Knee
7	Right Leg	G	Right Ankle
8	Right Foot	H	Left Hip
9	Left Thigh	I	Left Knee
10	Left Leg	J	Left Ankle
11	Left Foot	K	Right Shoulder
12	Right Upper Arm	L	Right Elbow
13	Right Forearm	M	Right Wrist
14	Right Hand	N	Left Shoulder
15	Left Upper Arm	O	Left Elbow
16	Left Forearm	P	Left Wrist
17	Left Hand		

Figure 18: Typical human body data set created by GEBOD.

GEBOD Program

GEBOD has two options for obtaining data sets for adult humans. The first, called adult human male or female option, allows the user to specify the gender and height and/or weight of the subject to be created. The second, user-supplied body dimensions option, allows the user to specify a set of thirty-two body dimensions for the subject to be created. A different method is used for each option to calculate the mass and geometric properties of adult humans.

USER-SUPPLIED BODY DIMENSIONS OPTION - The user-supplied body dimensions option computes the segment ellipsoid semiaxes and joint locations using expressions based on the anthropometric body dimensions supplied by the user. This approach assumes that, when the body is in a standing position with the arms at the sides, the joints are all in the same coronal plane and only the shoulder and hip joints are offset laterally. The ellipsoid centers are also assumed to be in the same plane. Except for the torso and feet, the mass properties for each segment are based on its ellipsoid volume. Basic geometric volumes derived from the user-supplied dimensions are used to calculate

the torso and feet segment mass properties. This technique assumes that the human body is homogeneous and therefore all body segments have the same density.

ADULT HUMAN MALE AND FEMALE OPTION - The adult human male and female option bases most of its calculations on Young's female[15] and McConville's male [16] stereophotometric surveys. These surveys provided three-dimensional, whole-body surface data as seen in Figure 19, which was segmented based on anatomical landmarks. The surface data for each subject were used to calculate the segment volumes, for determining the mass properties. GEBOD uses regression equations, based on height and weight, from these stereo studies to predict the segment mass properties. Again the body is assumed to be homogeneous with constant density between segments. Similar regression equations were developed for the joint center locations, which were referenced to the measured anatomical landmarks. Regression equations are also used to calculate the same thirty-two body dimensions in the user-supplied option. These calculated dimensions and the joint locations are used to determine the contact ellipsoid semiaxes and locations.

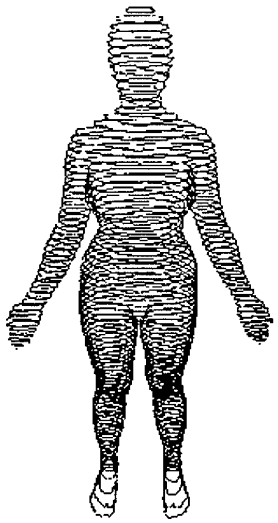

Figure 19: Typical stereophotometric data.

Validation with a manikin

In order to validate both the testing procedure and the ATB's calculation of the whole-body center of gravity and principal moments of inertia, a large ADAM (Advanced Dynamic Anthropomorphic Manikin) was disassembled at its articulations into its component segments. Each segment was measured to obtain its mass, principal moments of inertia, center of gravity location, joint locations, and surface dimensions, as well as the joint torque properties. These measurements were used to assemble an ATB model of the large ADAM[17]. The model has eighteen segments and seventeen joints.

The whole-body CG and principal MOI of a large ADAM were measured using the same procedure as was used for the human subjects. The positions of several points on the dummy were measured in the seat coordinate system with the electronic position coordinate digitizer. The ATB model of the large ADAM was precisely positioned using the measured ADAM points. The ATB program then calculated the whole-body CG and MOI. The ATB-predicted results compared very well with the measured values, as shown in Table 8.

Table 8: ADAM measured vs predicted.

		Principal MOI ($kg\text{-}cm^2$)	Center of Gravity (cm)
Measured Values	X:	99356	23.05
	Y:	102014	
	Z:	27597	26.05
ATB Predicted Values	X:	100347	23.27
	Y:	103843	
	Z:	26934	26.24
Percent Error	X:	-1.00%	-0.95%
	Y:	-1.79%	
	Z:	2.40%	-0.73%

Model Results

Two ATB input files were generated for each subject tested, one using the adult male or female option and one using the user-supplied dimensions option. In the first case, the measured height and weight of the subject was the input to GEBOD; in the other case, thirty-two anthropometric measurements were input. In all cases, a fifteen-segment model was created.

Initially, the linear and angular positions of the segments were determined using measurements taken during the testing process, similar to the method used with the ADAM. However, since it was desired to check the results of the entire, normal ATB modeling process, a different method of positioning the subject models was ultimately used. Three planar surfaces (planes) were defined to model the seat pan, seat back, and floor (Figure 20). Contacts between these planes and the body segments and between the segments were defined. The body models were positioned within the seat to closely approximate the position of the subject within the actual seat, and such that the segments were in static equilibrium. Equilibrium was achieved by positioning the model, running the ATB for time zero, and checking the initial linear and angular accelerations of each segment. Adjustments to the segment positions were made until the accelerations were acceptably low. The ATB program was then run to calculate the whole-body inertial properties.

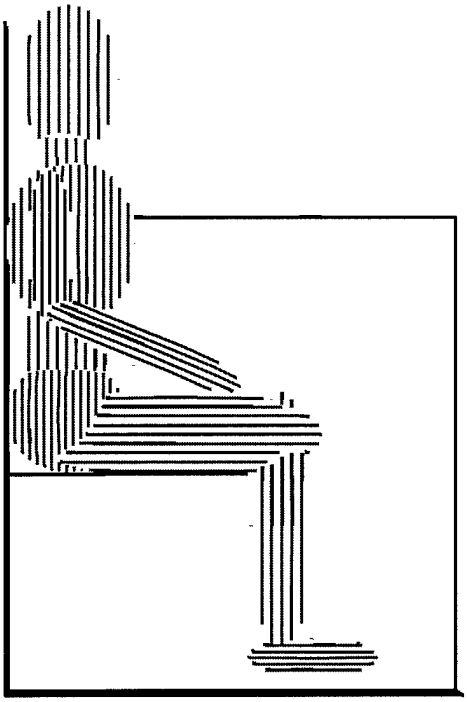

Figure 20: GEBOD data set positioned by ATB model in seat.

CENTER OF GRAVITY - The CG was found for each subject based on a coordinate system with the origin at the SRP. The measured data showed female subjects' CGs tend to be lower and further back as compared to the male subjects' CGs. For this reason female and male data have been separated when comparing measured and predicted CGs. Table 9 shows the averages of the differences in CG_x and CG_z between the measured data and those predicted using the two GEBOD options. On average, the adult human option had an error of about 1 cm for CG_x, while the user-supplied option had an average error of about 0.7 cm. For CG_z the adult option had an average error of 1.9 cm, while the user-supplied option had an average error of 5.0 cm. Figure 21 shows that both options over and under predict CG_x. CG_z is mainly under predicted, especially by the user-supplied option, as seen in Figure 22.

Table 9: Summary CG data.

Average Difference	N	Adult Option		User-Supplied	
		CG_x (cm)	CG_z (cm)	CG_x (cm)	CG_z (cm)
Total	69	0.97	1.85	0.65	5.04
Female	34	1.40	0.81	0.82	4.65
Male	35	0.56	2.87	0.49	5.43

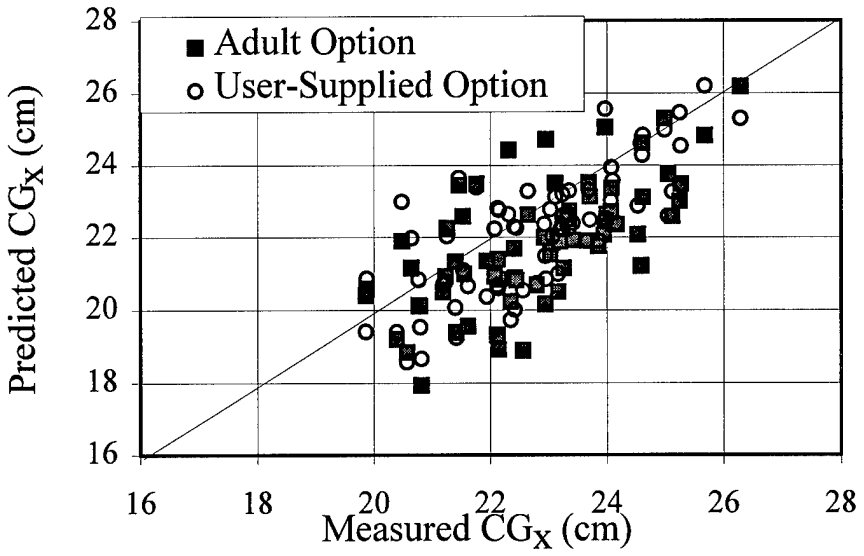

Figure 21: Measured and predicted CG_x locations.

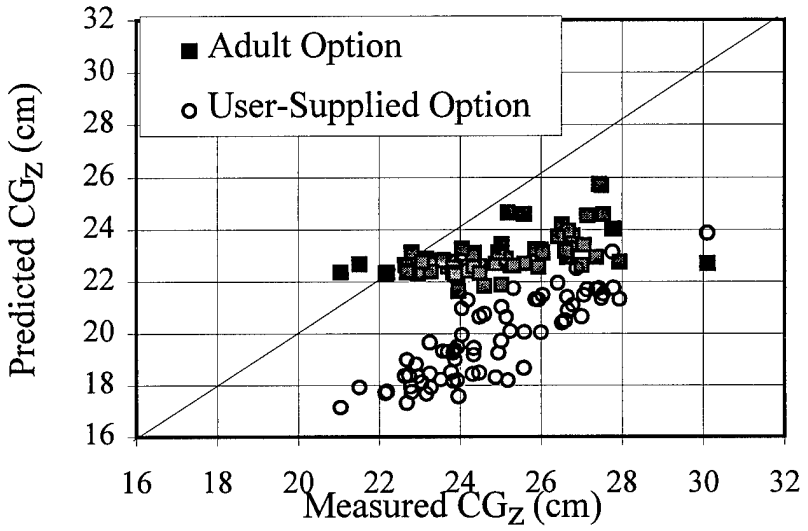

Figure 22: Measured and predicted CG_z locations.

Figures 23 and 24 show plots of all the CGs, females and males. On each plot, ellipses have been added around measured, adult option, and user-supplied points to illustrate the overall difference between the cases. This again indicates that the adult option does a better job of predicting CG_z than does the user-supplied option, but the user-supplied option better demonstrates the variability between subjects. The adult option has very little variability in predicting CG_z since it does not account for the differences in body proportions.

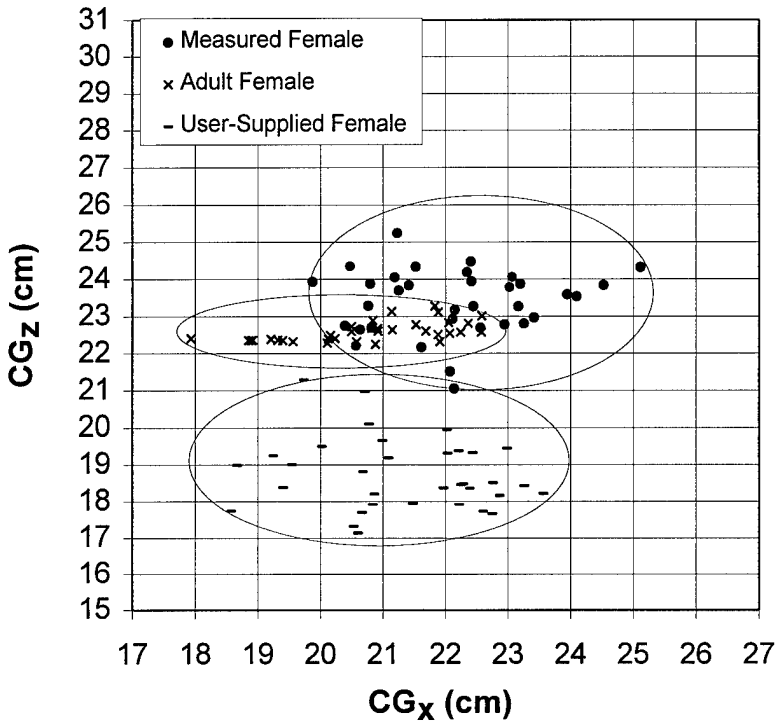

Figure 23: Female center of gravity locations.

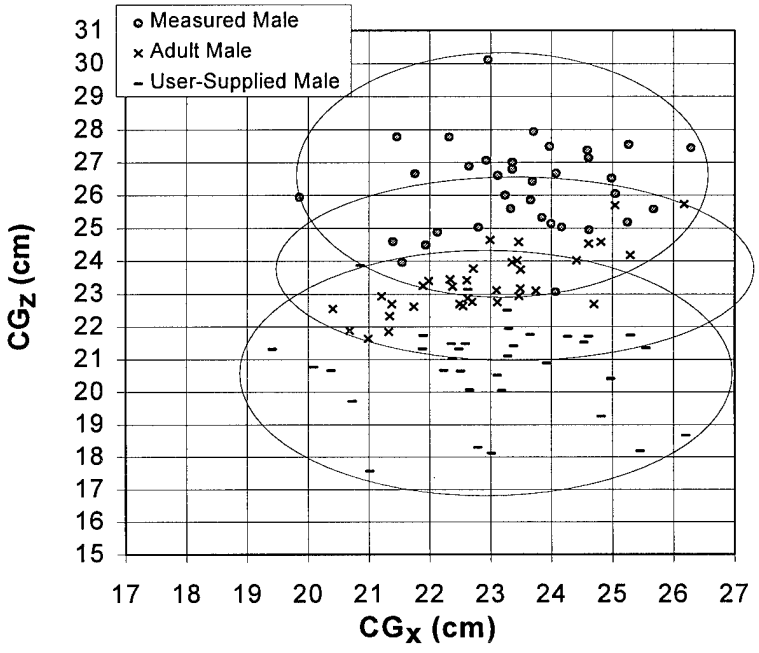

Figure 24: Male center of gravity locations.

MOMENTS OF INERTIA - The measured MOI data (X, Y, and Z principal moments through the center of gravity) are mainly dependent on mass and stature. There is no difference between males and females except that the females were usually smaller and therefore had smaller moments. Table 10 shows the average percent error in the X, Y, and Z moments between the measured data and the predicted using the two GEBOD options. On average the adult option had an error of about 15%, 16% and 18% for I_x, I_y and I_z, respectively. The user-supplied option had an average error of about 14%, 18%, and 23% for I_x, I_y, and I_z, respectively. Figures 25, 26 and 27 show plots of I_x, I_y, and I_z, respectively versus subject mass. These show that both options under predict all moments, with the adult option doing a slightly better job for I_y and I_z.

Table 10: Summary MOI data.

Avg Error (%)	N	Adult Option			User-Supplied		
		I_x	I_y	I_z	I_x	I_y	I_z
Total	69	15	16	18	14	18	23
Female	34	13	16	15	14	21	21
Male	35	17	16	21	13	16	25

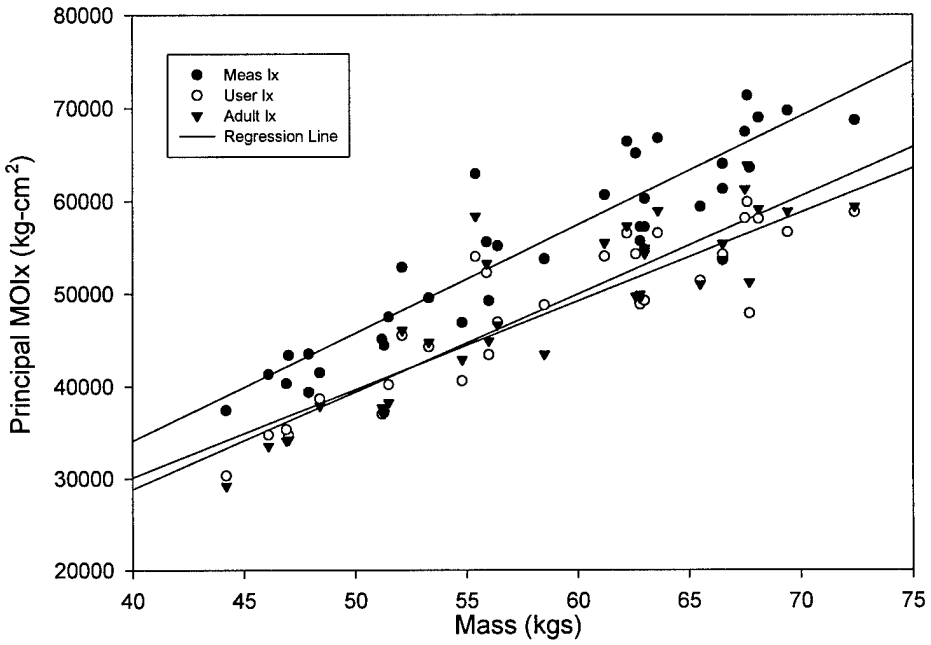

Figure 25: Measured and predicted principal MOI_x.

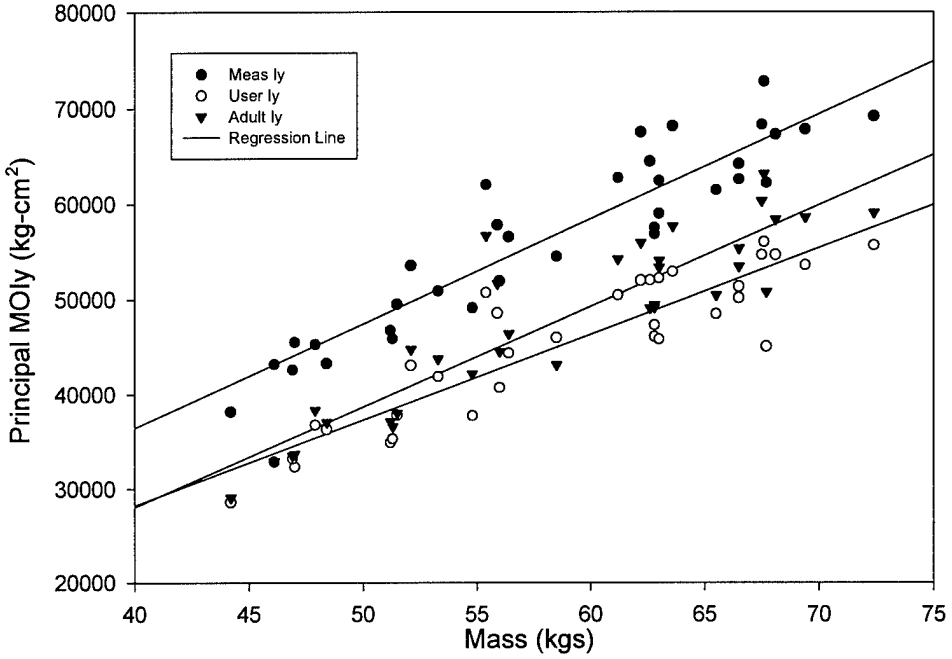

Figure 26: Measured and predicted principal MOI_y.

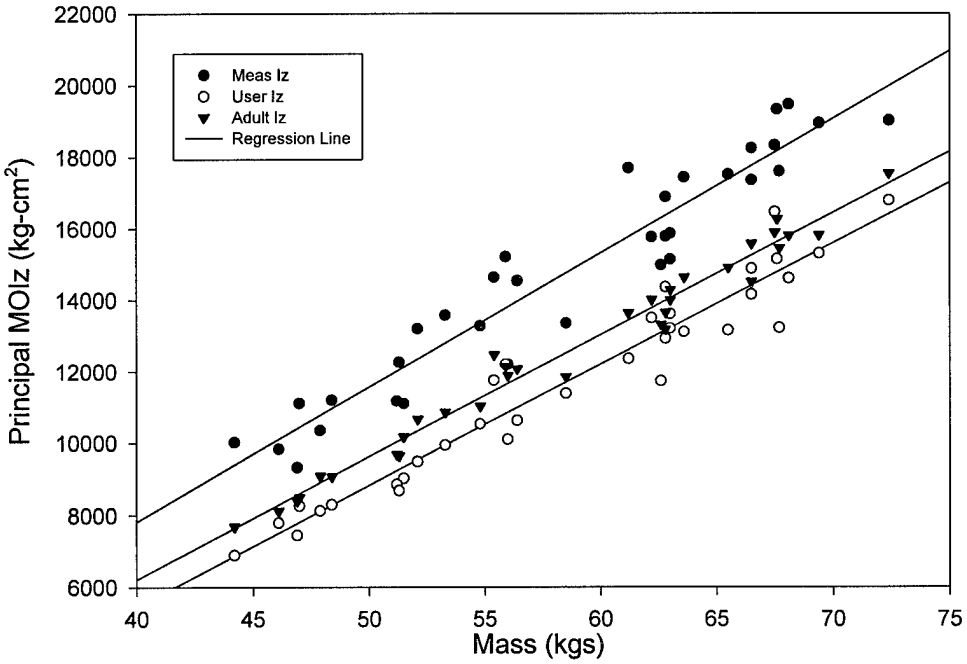

Figure 27: Measured and predicted principal MOI_z.

CONCLUSIONS

The whole-body mass properties testing methodology proved to be accurate and reliable for the test block, manikin, and human subject measurements. For the test block, the system accuracy was within 4%. Also, the coefficient of variance with human subjects was less than 2%. The manikin results verified the analytic procedure used in the ATB to obtain whole-body mass properties from the segmented body data set. The difference between measured and predicted center of gravity was less than 3 mm, and the moments of inertia varied by less than 3%.

While the predicted GEBOD mass properties are representative of the population trends seen in the human test data, there are significant differences in CG locations and MOI magnitudes. Both GEBOD options predicted the CG_x location within 1.5 cm, on average, and reflected the subject body size variability. The CG_z differences were much more significant, especially for the user-supplied option. However, because the user-supplied option takes into account specific body part dimensions, it resulted in CG_z scatter similar to that seen in the test data. Meanwhile, the adult human option, which only uses subject height and weight, predicts little variation in CG_z. The MOIs are consistently under predicted using both GEBOD options. The two larger moments, I_x and I_y, averaged 16% error, while I_z averaged 20% error. I_z is typically one-fourth the magnitude of I_x or I_y. In this case, both options demonstrated the population variability seen in the test data. There are a number of possible sources for the differences seen between the predicted and measured data. While the subjects were constrained as much as safely possible, some subject movement was evident, especially when they were moved between upright, reclined, and angled orientations. This primarily affected CG_z location, measured with the subjects in the reclined position. In this position, subjects frequently reported torso extension. Some minor errors may have resulted from variations between test and modeled individual body segment orientations. Positioning the body in the ATB program involved balancing the body weight against the seat pan. Therefore, the predicted CG_z locations are highly dependent upon the force-deflection properties defined for the contacts, and the lower torso and upper leg ellipsoid dimensions. The ellipsoid geometry is approximated by GEBOD based on limited body dimensions. These ellipsoids, particularly the center offset with respect to the segment CG, are likely to be inaccurate, causing poor positioning of the individual segment CGs within the seat. This positioning would have little effect on MOI predictions. In the user-supplied option, the simplified geometric shapes, used to calculate segment volumes, could cause error in the calculated mass properties. Finally, in both options, the constant density assumption does not account for mass distribution variability within and between segments.

Based on this study, several directions are being considered for improving GEBOD mass property predictions. The ellipsoid geometries will be reviewed and adjusted based on this study's findings and other available data. The adult human option, which uses more detailed body surface data to calculate the segment mass properties, provides better overall predictions than does the user-supplied option. Therefore, the use of whole-body

3-D laser scanning, providing more accurate surface data, may further improve volume prediction. Also allowing the adult human option to use additional subject body dimensions would increase its ability to account for body proportion variability. Testing of subjects in different body segment orientations (i.e., seated with legs straight forward, prone, etc.) would allow individual segment properties to be derived from the differences in the whole-body measurements and would provide insight into the density variation between segments. For example, increasing the head and foot density and reducing the torso density would increase the whole-body MOI. The homogeneous density assumption can also be investigated using modern imaging techniques, providing insight on mass distribution throughout the body. The possible benefits of several of these approaches will be explored analytically using the ATB model.

It is important to recognize that the validity of the GEBOD generated human body data sets is dependent upon the user's application. This study's results show errors in whole-body mass properties that may have significant effects on controlled-propulsion ejection seat design. However, the CG and MOI errors are small compared to the range seen within the population and are less than variations seen due to positioning or body motion within an ejection seat[18]. For other applications in which whole-body inertial properties are not of interest, such as predictions of body dynamics in impact events, earlier validation studies have demonstrated that the errors in mass distribution may not have significant effect on simulation results.

REFERENCES

1. Defense Authorization Act 260.9B.

2. Congressional Record-House (H9436), dated 10 November 1993.

3. Rasmussen, R.R., Jr., "Test Plan: Human Center of Gravity and Mass Moments, Work Unit 72313601, January 1995.

4. McConville, John T., Churchill, T.D., Kaleps, I., Clauser, C.E., and Cuzzi, J., "Anthropometric Relationships of Body and Body Segment Moment of Inertia," AFAMRL-TR-80-119 (AD A097 238), Aerospace Medical Research Laboratory, WPAFB, Ohio, 1980.

5. Obergefell, L., Ma, D., Rizer, A., and Andries, M., "Leg Clearance Predictions Using Ejection Simulations," SAFE Proceedings, Reno NV, October 1996.

6. Schultz, R.B., "Whole-Body Center of Gravity and Moments of Inertia Study," Defense Women's Health Research Program - Proposal, Armstrong Laboratory (AFMC), Brooks AFB, Texas, September 1995.

7. Bjorn, V., Research Protocol #95-03 for Human Center-of-Gravity and Mass Moments of inertia, February 1995.

8. Baughn, D.J., Albery, C.A., and Kaleps, I., "The Standard Automated Mass Properties (STAMP) Testing and Calibration Procedures," AL/CF-TR-1995-0091, Armstrong Laboratory (AFMC), WPAFB, Ohio, 1995.

9. Gordon, C.C., Bradtmiller, B., Clauser, C., Churchill, T. McConville, J.T., Tebbetts, I., and Walker, R., "1987-1988 Anthropometric Survey of U.S. Army Personnel: Methods and Summary Statistics", NATICK/TR-89-044, U.S. Army Matick Research, Development, and Engineering Center, Natick, MA, 1989.

10. Lim, Czer A and Rebecca B. Schultz, Variability Assessment for the Whole-Body Center of Gravity and Moment of Inertia Study, Final Report for 1996 NASA Sharp Plus Program Central State University, August 1996.

11. Marsh, Mary Virginia, Thesis: Computational Analysis of Whole Body Inertia Properties, The University of Alabama, August 1996.

12. Cheng, H., Obergefell, L.A., and Rizer, A.L., "Generator of Body Data (GEBOD) Manual," Armstrong Laboratory Report No. AL/CF-TR-1994-0051, WPAFB Ohio, March 1994

13. Obergefell, L.A., Gardner, T.R., Kaleps, I., and Fleck, J.T., "Articulated Total Body Model Enhancements, Volume 2: Users' Guide," Harry G. Armstrong Aerospace Medical Research Laboratory Report No. AAMRL-TR-88-043, WPAFB Ohio, January 1988.

14. Lupker, H.A., de Coo, P.J.A., Nieboer, J.J., and Wismans, J., "Advances in MADYMO Crash Simulations," SAE 910879, Proceedings SP-851, International Congress and Exposition, Detroit MI, Society of Automotive Engineers, 1991.

15. Young, J.W., Chandler, R.F., Snow, C.C., Robinette, K.M., Zehner, G.F. and Lofberg, M.S., "Anthropometric and Mass Distribution Characteristics of Adult Females," FAA-AM-83-16, Office of Aviation Medicine, Federal Aviation Administration, Oklahoma City OK, 1983.

16. McConville, J.T., Churchill, T.D., Kaleps, I., Clauser, C.E., and Cuzzi, J., "Anthropometric Relationships of Body and Body Segment Moments of Inertia," AMRL-TR-80-119 (AD A097 238), Aerospace Medical Research Laboratory, WPAFB OH, 1980.

17. Rizer, A.L., Obergefell, L.A., Johnson, D., Thompson, G., "Development of a Simulation Database for the Advanced Dynamic Anthropomorphic Manikin (ADAM)," Proceedings of the 32nd Annual Symposium SAFE Association, Reno NV, 1994.

18. Obergefell L., and Kaleps, I., "Simulation of Body Motion During Aircraft Ejection," Mathematical Modelling in Science and Technology, The Sixth International Conference, August 1987.

List of publications and abstracts:

Abstract, presentation and publication in proceedings:

> "Measurement of Whole-Body Human Center of Gravity and Moments of Inertia," R. Schultz, C. Albery, and D. Banks, 34th Annual SAFE Symposium, Reno NV, 21-23 October 1996.

Abstract, presentation and publication (in 1997)

> "Human Whole-Body Center of Gravity and Moments of Inertia," R. Schultz, I. Kaleps, V. Bjorn, and G. Zehner, 68th Annual Scientific Meeting, Aerospace Medical Association, Chicago IL, 11-15 May 1997.

Abstract, paper (draft submitted) and presentation (awaiting acceptance)

"Comparison of Measured and Predicted Human Whole-Body Inertial Properties", R. Schultz, L.A. Obergefell, A.L. Rizer, C.B. Albery, A. Anderson, 41st Stapp Car Crash Conference, Lake Buena Vista, FL, 12-14 November 1997.

List of people receiving salary for working on project:

Capt Rebecca Schultz
Lt Daryl Banks
Edward Eveland
Doug Frank
Chris Albery
Greg Thompson
Greg Zehner
Judy Lee
Sherry Blackwell
Tina Brill
Virginia Marsh